

## Investigation of Inductor Poles Shape Influence on Magnetic Field Distribution

R. Lukočius, M. Šiožinys

Department of Electrical Engineering, Kaunas University of Technology,

Studentų str. 48, LT-51367, Kaunas, Lithuania, phone: +370-652-25572, e-mail: milvydas.siozinys@gmail.com

V. Šiožinys

Department of Electric Power Systems, Kaunas University of Technology,

Studentu str. 48, LT – 51367, Kaunas, Lithuania, phone: +370-652-37826, e-mail: vytautas.siozinys@gmail.com

### Introduction

Rotary magnetic fields are being used in numerous industrial processes related to mach the hard powdery materials, hard-fluid and hard-gaseous systems in processes of synthesis of new products, in processes of mass exchange drying mixing, etc [1–7]. The following phenomena may occur under the action of magnetic field: changes of the heat conductance of the material division of heterogeneous medium. Generation of electric current in the closed circuit at the condition of moving conducting fluids in the magnetic field changes due to the properties of magnetized media [6, 7].

The problems of creations uniform rotary magnetic field in all air gap of active zone are different from the problems of electric fields in the electric motor due to of the difference of processes in moving parts [4, 5].

The requirements for the rotating magnetic field inductor are different for the process activating units used for different purposes. However, there are some common inductors properties for technological rotating magnetic field:

1. The active zone is created in the tube with diameter not less then  $D = 50 \div 100$  mm, as described [2, 3]. Therefore the air gap is very big.

2. The magnetic flux density equal to  $0.1 \div 0.2$  T must be created in this air gap. The considerable power for such magnetic field excitation is needed and solely the three-phase inductors are used [1].

3. The uniform value of the magnetic flux density is desirable in the all active zone. It is particularly important for process activating units without the vortex ferromagnetic layer.

The mean magnetic flux density and mean magnetic flux values should be investigated inside inductor incase of ferromagnetic materials are not used in active zone. Each

calculation should be performed for the same coil current density value for proper comparison of the results.

### Mathematical background

The aim of this paper is numerical simulation of salient-pole inductor (Fig. 1). Computation area is two-dimensional. Coils U, V and W are excited by symmetrical three-phase current system:

$$\begin{cases} i_U = I_m \sin(\omega t + \psi_i), \\ i_V = I_m \sin(\omega t + \psi_i - 120^\circ), \\ i_W = I_m \sin(\omega t + \psi_i + 120^\circ), \end{cases} \quad (1)$$

here  $\psi_i$  is current initial phase,  $I_m$  is current magnitude. Pairs of poles are shifted on a circle of an inductor by  $120^\circ$ . Stroke-through area of magnetic circuit cross section in Fig. 1 represents the electric steel of magnetic circuit.

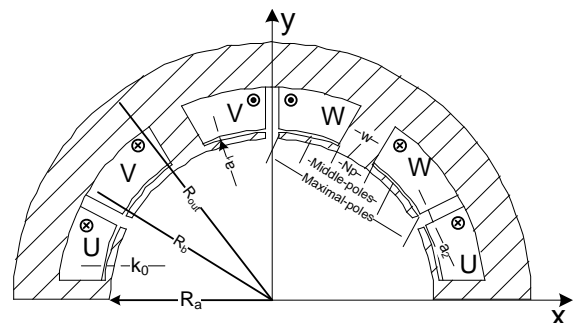


Fig. 1. The view of inductor cross section

Numerical simulation of two-dimensional magnetic field of an inductor is performed using the program COMSOL Multiphysics. Governing equation of the field is the following

$$\nabla \times (\mu_0^{-1} \mu_r^{-1} \nabla \times A) = \mathbf{J}_z^e e_z, \quad (2)$$

here  $A$  – the vector magnetic potential;  $J$  – external current density  $z$  component;  $\mu_0$  is permeability of vacuum;  $\mu_r$  is magnetic permeability.

Current density in each coil of the pole (Fig. 1) is linearly dependent on the current  $i$

$$J = \frac{i \cdot N}{S}, \quad (3)$$

here  $N$  – number of turns in the unit area of cross section of the coil,  $S$  – an area of cross section of the coil.

The coil fill factor is not evaluated in the article. Substituting values of phase currents from (1) into (3) values of current density may be determined for each instant of time.

The rotational magnetic field is computed using eq. (2). The magnetic flux density mean value in the active zone is concerned with relative active zone diameter  $D_a / D$  which value varies in some range. Here  $D_a$  is the distance between the contrary poles and  $D = 2 \cdot R_a$  is the active zone diameter as depicted in Fig. 1.

The calculation results are presented as the function of magnetic flux density and relative active zone diameter to demonstrate the dispersion of magnetic flux density along axis  $x$ . The mean value of magnetic flux density  $\bar{B}_m$  is evaluated using

$$\bar{B}_m = \frac{1}{n} \sum_{i=1}^n B_i, \quad (4)$$

here  $B_i$  – the active zone magnetic flux density for each time moment.

The dissipation of magnetic flux density along active zone is described by magnetic flux density dispersion

$$S^2(B_i) = \frac{1}{n-1} \sum_{i=1}^n (B_i - \bar{B}_m)^2. \quad (5)$$

Farther on are represented investigations of the inductor geometry parameter  $k_0$  influence to the mean value of the magnetic flux density.

### Investigation of influence of poles dimensions to the circumferential direction

The parameters of model in Fig. 1 are:  $R_a = 50$  mm,  $R_b = 66$  mm,  $R_{out} = 80$  mm,  $w = 12$  mm,  $a_1 = 2$  mm,  $a_2 = 2$  mm,  $k_0 = 2$  mm.

Relative permeability of steel is  $\mu_r = 1000$ . The magnitude of phase current  $I_m = 4$  A, the number of turns in each pole phase winding is 1000. The calculations are performed in time range of  $0 \div 0.02$  s using time step  $0.001$  s.

There was investigated the magnetic field distribution in the active zone for three different poles dimensions in the circumferential direction Fig. 1: for the non-salient

poles, for the middle length poles and for the maximal length poles.

Simulations of the three cases (where the current density in each model are the same):

1.  $k = k_0$  and  $R = R_a$ .
2.  $k = 2 \cdot k_0$  and  $R = R_a$ .
3.  $k = 4 \cdot k_0$  and  $R = R_a$ .

### Simulation results

The modeling results are rotating magnetic field which the magnetic flux values depends on relative active zone diameter  $D_a / D$ .

The Fig. 2 to 4 depicts magnetic flux density in active zone for parameters value of  $k = k_0$  and  $R = R_a$ .

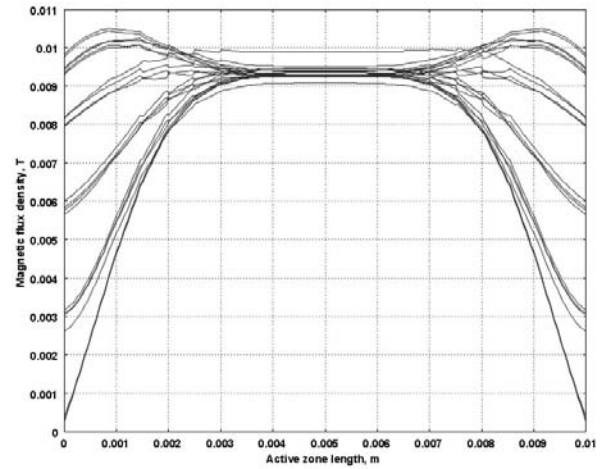


**Fig. 2.** Simulation results of magnetic flux density in the active cylinder zone for maximal poles inductor for the each time step. The active zone is limited by relative diameter  $D_a / D = 1$

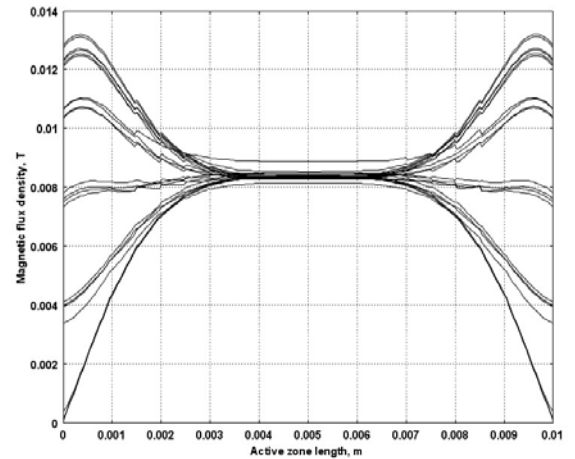


**Fig. 3.** Simulation results of magnetic flux density in the active cylinder zone for middle poles inductor for the each time step. The active zone is limited by relative diameter  $D_a / D = 1$

The dependences of active zone magnetic flux mean value and dispersion from active zone dimension  $k = k_0$  and  $R = R_a$  are introduced in Table 1.

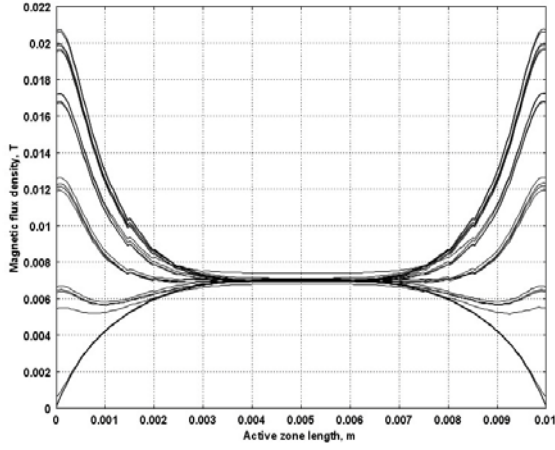


**Fig. 4.** Simulation results of magnetic flux density in the active cylinder zone for non-salient poles inductor for the each time step. The active zone is limited by relative diameter  $D_a / D = 1$

**Table 1.** The maximal and minimal values of magnetic flux density in the active zone cylinder limited by relative diameter  $D_a/D$  ( $k=k_0$ )

$D_a/D$	Maximal poles		Middle poles		Non-salient poles	
	$\bar{B}_m$	$S^2(B_i)$	$\bar{B}_m$	$S^2(B_i)$	$\bar{B}_m$	$S^2(B_i)$
mm	mT	nT	mT	nT	mT	nT
0.2	9.344	23.872	8.39	19.286	7.008	13.466
0.3	9.342	24.519	8.391	20.146	7.009	14.143
0.4	9.339	28.822	8.394	26.008	7.015	19.758
0.5	9.325	48.196	8.398	54.470	7.030	46.282
0.6	9.285	118.366	8.404	152.775	7.066	146.685
0.7	9.203	331.117	8.414	435.214	7.147	481.546

**Table 2.** The maximal and minimal values of magnetic flux density in the active zone cylinder limited by relative diameter  $D_a/D$  ( $k = 2 \cdot k_0$ )

$D_a/D$	Maximal poles		Middle poles		Non-salient poles	
	$\bar{B}_m$	$S^2(B_i)$	$\bar{B}_m$	$S^2(B_i)$	$\bar{B}_m$	$S^2(B_i)$
mm	mT	nT	mT	nT	mT	nT
0.2	10.171	28.308	9.367	24.032	7.916	17.174
0.3	10.169	29.104	9.366	24.980	7.916	17.947
0.4	10.163	33.759	9.365	30.870	7.918	22.826
0.5	10.145	56.037	9.362	58.619	7.926	47.019
0.6	10.100	140.757	9.357	159.829	7.954	145.439
0.7	10.009	397.536	9.349	457.615	8.023	474.890

The highest magnetic flux density values are reached for wide pole inductor with active zone width  $D_a = 20$  mm as described in Table 1. On other hand, the smallest magnetic flux density value generate non-silent pole inductor in the active zone  $D_a/D = 0.2; 0.3; 0.4$  mm.

The active zone diameter  $D$  decreases if the pole parameter  $k$  increases to  $2 \cdot k_0$  or  $4 \cdot k_0$  for inductor

construction depicted in Fig. 1. The inductor geometry increases to the value  $R = R_a$  to satisfy model initial conditions equal for all calculation examples. The increase of coil area requires change the coil number of windings as could be seen from (3) respectively  $N \cong 1092$  for ( $k = 2 \cdot k_0$ ) and  $N \cong 1291$  for ( $k = 4 \cdot k_0$ ). The mean magnetic flux density and dispersion values for active zone diameter and pole parameters  $k = 2 \cdot k_0$  and  $k = 4 \cdot k_0$  respectively are shown in Table 2 and 3.

**Table 3.** The maximal and minimal values of magnetic flux density in the active zone cylinder limited by relative diameter  $D_a/D$  ( $k = 4 \cdot k_0$ )

$D_a/D$	Maximal poles		Middle poles		Non-salient poles	
	$\bar{B}_m$	$S^2(B_i)$	$\bar{B}_m$	$S^2(B_i)$	$\bar{B}_m$	$S^2(B_i)$
mm	mT	nT	mT	nT	mT	nT
0.2	11.898	38.743	11.547	36.495	9.957	27.121
0.3	11.896	39.856	11.546	37.609	9.956	28.050
0.4	11.888	46.441	11.543	44.120	9.957	33.681
0.5	11.868	78.284	11.539	76.918	9.966	62.015
0.6	11.815	199.263	11.529	197.320	10.000	188.667
0.7	11.703	561.513	11.502	544.792	10.759	598.034

The highest magnetic flux mean values are reached for wide pole inductor construction with ( $k = 4 \cdot k_0$ ) and active zone diameter  $D_a = 20$  mm. However the dispersion of magnetic flux density is also the highest.

### Magnetic flux distribution in the cylinder form active zone

The magnetic flux in circle area is calculated for each relative diameter  $D_a/D$  in active zone. For that purpose, the equation was involved

$$\Phi_{D/D_a} = \int_S \vec{B}_{\text{norm}} \cdot \vec{dS} \quad (6)$$

The mean magnetic flux values for the same active zone area for investigated time interval were calculated

$$M_{\Phi_{D/D_a}} = \frac{1}{n(\Delta t)} \sum_{t=0}^n \Phi_{D/D_a}(t), \quad (7)$$

here  $t$  – time step.

The calculation results of mean magnetic flux values dependency of relative active zone diameter are depicted in Fig. 5. The changes of inductor poles construction parameter  $k$  by step  $k_0, 2 \cdot k_0, 4 \cdot k_0$  changes the mean magnetic flux in the investigated area.

The increase of mean of magnetic flux could be seen at the inductor pole plane. The smallest value of magnetic flux is reached for the non-salient inductor construction for  $k = 2 \cdot k_0$  at the active area equal to  $D_m = D_{0.2} + D_{0.3}$ .

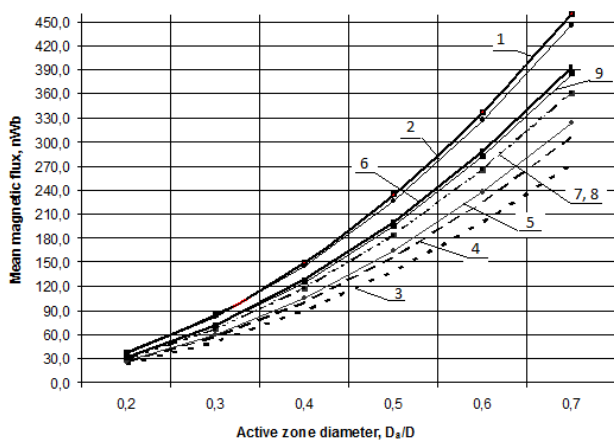


**Fig. 5.** The mean magnetic flux value dependency on relative active zone diameter  $D_a / D$ : 1) maximal poles  $k = 4 \cdot k_0$ ; 2) middle poles  $k = 4 \cdot k_0$ ; 3) non – salient poles  $k = k_0$ ; 4) non – salient poles  $k = 2 \cdot k_0$ ; 5) middle poles  $k = k_0$ ; 6) maximal poles  $k = 2 \cdot k_0$ ; 7) middle poles  $k = 2 \cdot k_0$ ; 8) maximal poles  $k = k_0$ ; 9) non – salient poles  $k = 4 \cdot k_0$

## Conclusions

1. The rotational magnetic flux and density vary and depends on inductor geometry.

2. The highest magnetic flux density is reached for the wide pole inductor with construction parameter  $k = 4 \cdot k_0$ . For such inductor construction type the highest flux density is reached for relative active zone diameter  $D_a/D = 0.2 \div 0.7$  mm.

3. The magnetic flux density dispersion vary in range from 22.34% to 87.58% due to changes of inductor pole parameter  $k = (1;2;4) \cdot k_0$  for the active zone  $D_s = 0.2 \div 0.4$ .

## References

1. **Romaškevičius O., Šiožinys M., Virbalis J.A.** The Influence of Exciting Current Unbalance to Parameters of Rotating Magnetic Field // *Electronics and Electrical engineering*. – 2008. – No. 3(83). – P. 85 – 88.
2. **Romaškevičius O., Šiožinys M., Virbalis J. A.** The Investigation of Poles Shape of the Technological Rotating Magnetic Field Inductor // *Electronics and Electrical engineering*. – 2010. – No. 5(101). – P. 17 – 20
3. **Šiožinys M., Žebrauskas S.** Simulation of magnetic field in rotary field inductor // *Proceedings of the International Conference „Electrical and Control Technology – 2010“*, Kaunas, 2010. – P. 269 – 272.
4. **Grainys A., Novickij J.** The Investigation of 3D Magnetic Field Distribution in Multilayer Coils // *Electronics and Electrical engineering*. – Kaunas: Technologija, 2010. – No. 7(013). – P. 9–12.
5. **Boudiaf A.** Numerical Magnetic Field Computation in a Unilateral Linear Asynchronous Motor without Inverse Magnetic Circuit // *Electronics and Electrical Engineering – Kaunas: Technologija*. – 2009. – No. 2(90). – P. 81–84.
6. **Bartkevičius S., Novickij J.** The Investigation of Magnetic Field Distribution of Dual Coil Pulsed Magnet // *Electronics and Electrical Engineering*. – Kaunas: Technologija, 2009. – No. 4(92). – P. 23–26.
7. **Промтов М. А.** Машины и аппараты с импульсными энергетическими воздействиями на обрабатываемые вещества. – Москва, Машиностроение, 2004. – 430 с.

Received 2010 10 18

**R. Lukočius, M. Šiožinys, V. Šiožinys.** Investigation of Inductor Poles Shape Influence on Magnetic Field Distribution // *Electronics and Electrical Engineering*. – Kaunas: Technologija, 2010. – No. 10(106). – P. 17–20.

The two dimensional magneto static problems are calculated using finite element method. The 6 non–silent pole inductor construction and coil current produced magnetic field is investigated. The step of time moments of symmetrical three–phase current system is 0.001 s. and the computation is performed for the time range  $0 \div 0.02$  s. The distribution of magnetic flux density value along axis x is investigated. The active zone mean magnetic flux density value and dispersion are calculated along axis x for each time moment. Concentric circle area magnetic flux mean values are calculated. The calculation results could be used to construct the required parameters inductors. Ill. 5, bibl. 7, tabl. 3 (in English; abstracts in English and Lithuanian).

**R. Lukočius, M. Šiožinys, V. Šiožinys.** Induktoriaus polių formos įtaka magnetinio lauko pasiskirstymui // *Elektronika ir elektrotechnika*. – Kaunas: Technologija, 2010. – Nr. 10(106). – P. 17–20.

Baigtinių elementų metodu dvimatėje erdvėje modeliuojamas magnetostatinis laukas. Nagrinėjamas šešių neišreikštų polių induktoriaus ričių kuriamas magnetinis laukas. Induktorius maitinamas trifaziu simetriniu srovės šaltiniu, modeliavimo trukmė  $0 \div 0,02$  s, laiko žingsnelis – 0,001 s. Tiriamas magnetinio srauto tankio reikšmės pasiskirstymas x ašies kryptimi. Skaičiuojama induktoriaus aktyviojoje zonoje kuriama vidutinė magnetinio srauto tankio ir dispersijos reikšmė x ašies kryptimi kiekvieną laiko akimirką. Skaičiuojama vidutinė magnetinio srauto reikšmė, apribota aktyviosios zonos koncentrinu apskritimo plotu. Modeliavimo rezultatai gali būti panaudoti, konstruojant tam tikrų parametru induktorių. Il. 5, bibl. 7, lent. 3 (anglų kalba; santraukos anglų ir lietuvių k.).